Journal of Photochemistry and Photobiology A: Chemistry 211 (2010) 78–87

Contents lists available at ScienceDirect

Journal of Photochemistry and Photobiology A: Chemistry

journal homepage: www.elsevier.com/locate/jphotochem

Photochemistry of photoresists and underlayer materials upon irradiation at 13.5 nm

Grace H. Ho*, Yu-H. Shih, Fu-H. Kang, Jia-C. Hung, Chih-H. Shao, Yu-H. Lai

Department of Applied Chemistry, National University of Kaohsiung, No. 700, Kaohsiung University Road, Nanzih, Kaohsiung 811, Taiwan

ARTICLE INFO

Article history:
Received 23 October 2009
Received in revised form 4 February 2010
Accepted 12 February 2010
Available online 21 February 2010

Keywords:
Extreme ultraviolet (EUV)
13.5 nm
Ionic outgassing
Pressure rise
Photoresist
Underlayer material

ABSTRACT

We measured the absolute ionic outgassing yield (AIOY) with a double-ion chamber method, characterized the outgassed ion species, derived the relative extent of outgassing F^+, CH_3^+ and $C_2H_5^+$ ions, determined the exposure rate constant for the formation of F^+ and CH_3^+ with a quadrupole mass filter, and monitored the relative pressure rise with an ion gauge. These experiments were performed with radiation at wavelength 13.5 nm from the synchrotron beamline 08A1BM-LSGM at National Synchrotron Radiation Research Center in Taiwan. Samples investigated included the round-robin resist, poly(methylmethacrylate), and twelve underlayer materials. The photochemistry in the extreme ultraviolet region of the fourteen samples is described according to the following results. The AIOY values, of order 10^{-3}, are proportional to the absorption coefficients of the samples. The extent of F^+ outgassing is related directly to the extent of F photoabsorption by the samples. Outgassing of CH_3^+ and $C_2H_5^+$ ions depends strongly on the type of polymer; the CH_3^+ outgassing and relative pressure rise both depend on a parameter related to photoabsorption at 13.5 nm and the polymeric structure of the sample. Dill's C parameter for CH_3^+ outgassing is identified to depend on the polymer type, whereas that for F^+ outgassing depends on the fluorine-containing moiety. Reaction mechanisms of EUV photochemistry are proposed according to the experimental results.

1. Introduction

Resist outgassing has been attributed to a possible source leading to extreme ultraviolet (EUV) optics contamination, subsequently hampering EUV lithography in high-volume manufacturing (HMV). Sematech (Semiconductor manufacturing Technology, USA) organized a benchmarking outgassing test on an EUV model resist (round-robin resist) of ESCAP (environmentally stable chemical amplification positive resist) type, and showed that the rate of outgassing determined in eight institutes differed by four orders of magnitude involving use of three experimental techniques—pressure rise, thermal desorption (TD)/gas chromatograph (GC)/mass spectrometry (MS), and quadrupole mass spectrometry (QMS) [1]. Researchers at SELETE (Semiconductor leading edge technologies, Japan) who tried to determine outgassing in quantity by the pressure rise method demonstrated a factor two in measurement precision using two vacuum-chamber systems and two light sources. The keys to achieving the experimental precision included summing the pressure rises for a given exposure dose and taking the pumping speed of each vacuum-chamber into account [2–5]. Moreover, those researchers showed an order of magnitude reduction in differences between the pressure rise and TD/GC–MS methods by considering the detection sensitivity of pressure ion gauge and collection efficiency for various samples by TD as additional compensation factors [5].

The effect of resist outgassing leading to contamination of EUV optics is still debated. NIST (National institute of standards and technology, USA) reported observable carbon contamination on a TiO_2-capped plate from several gaseous organic samples with a rate of deposition that is describable with the molecular adsorption–desorption Temkin model [6]. ASML, a provider of lithography systems, reported an improved vacuum as an effective means to decrease carbon contamination on optics under HVM conditions, and suggested strict selection of materials to mitigate contamination [7]. Sematech announced a halt of the resist-outgassing test at their microexposure tool for conventional PAG resists, because evidence is lacking that resist outgassing produced optic contamination under conditions of low-power exposure for EUV scanners [8].

Interestingly, most outgassing studies either examined hydrocarbon outgassing to set the outgassing limit [8–11] or used the detection method with TD/GC/MS or pressure rise [1–6,12–14], which can detect only stable and neutral species. Among many investigations of resist outgassing, reactive species such as F, HF, CF_2, CF_2H and other F-containing radicals from PAG have been iden-

* Corresponding author. Tel.: +886 7 5919459; fax: +886 7 5919348.
E-mail address: graceho@nuk.edu.tw (G.H. Ho).

1010-6030/$ – see front matter © 2010 Elsevier B.V. All rights reserved.
doi:10.1016/j.jphotochem.2010.02.008

tified qualitatively only a few times with the QMS method as minor products [3,15–17].

We performed the first investigation of ionic outgassing on photoacid generators (PAG), and identified reactive F^+, $C_xF_y^+$ and $C_nH_m^+$ as important ionic outgassed species [18]. The role of ionic outgassing on the EUV optic contamination has largely been neglected, regardless of the fact that photons with energy 91.84 eV (wavelength 13.5 nm) ionize all materials with a quantum yield generally close to or greater than unity; ion–molecule reactions proceed near collision rates [19–23]; and that F-etch or F-assisted erosion or oxidation are common reactions for etching wafers [24]. Researchers at IMEC (an independent research center in nano-electronics and nano-technology in Europe) first reported the importance of F-contamination. In that study, carbon and fluorine contamination were observed in a comparable amount on the surface of a witness plate by using surface sensitive X-ray photoelectron spectroscopy [25]. Contradicting an environmental concern seeking a decreased use of perfluoroalkylsulfonate (PFAS) compounds [11], a strategy to increase EUV resist sensitivity is to enhance photoabsorption with additional fluorination of EUV photoresists. An incremental fluorination has been demonstrated theoretically and experimentally to be a feasible approach to improve the problems of resist sensitivity/resolution/line-edge-roughness tradeoff without sidewall degradation [17,26–28].

As outgassing of fluorine-containing neutral molecules has been rarely reported; little work on ionic outgassing but dominant F^+ and $C_xF_y^+$ outgassing from photoacid generators, and the recent and first observation of F-contamination by the witness plate method inspire our detailed investigation of ionic outgassing. We determine the absolute ionic outgassing yield from two photoresists and twelve underlayer materials upon irradiation at 13.5 nm. The outgassed ions are also characterized. Additionally, F^+, CH_3^+, and $C_2H_5^+$ outgassing are quantified to a relative extent, as well as a pressure rise. Moreover, rate constants and Dill's C parameters leading to F^+ and CH_3^+ formation are determined. Based on the results of this study, reaction mechanisms for EUV photochemistry are proposed.

2. Experiments

Light at 13.5 nm was delivered from beamline 08A1BM-LSGM at National Synchrotron Radiation Research Center. Fourteen samples here include polymethylmethacrylate (PMMA, $(C_5H_8O_2)_n$); the model EUV round-robin resist, which is denoted RRR in this study and consists of 94% poly(4-hydroxystyrene-co-*tert*-butyl acrylate) in 60–40 copolymerization, 5% di(tert-butylphenyl)iodonium-1-perfluorobutanesulfonate, and 1% tetrabutylammonium hydroxide; and twelve EUV underlayer materials (UL): three UL-polyesters (UL-1A to -1C), three UL-novolacs (UL-2A to -2C), three UL-PAG-attached-methacrylates (UL-3A to -3C), and three UL-methacrylates (UL-4A to 4-C). The samples were provided by Nissan Chemical Industries, Ltd. (NCI); the stated thickness of PMMA, RRR, and the UL samples on wafers are 125, 125, and 30 nm, respectively. Additional information about UL compositions is provided here only as required, as this information is the intellectual property of NCI.

2.1. Absolute ionic outgassing yield

We use a double-ion chamber method to determine the absolute ionic outgassing yield (AIOY) of PMMA, RRR, and UL materials upon irradiation at 13.5 nm. To our knowledge, this study is the first to evaluate AIOY from a thin-film photoresist and UL samples at that wavelength. The details of the double-ion chamber method that encloses a photoabsorption cell to determine absolute photoabsorption and photoionization quantities of gaseous

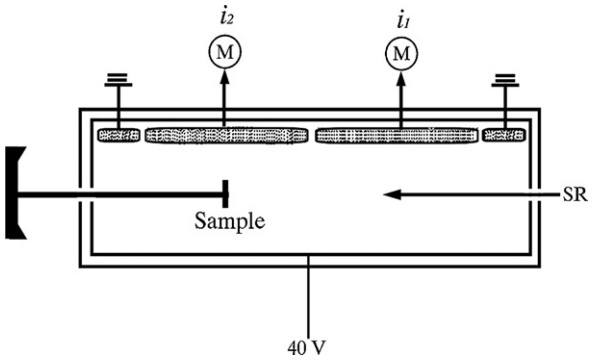

Fig. 1. Double-ion chamber apparatus for AIOY measurements.

samples are available elsewhere [19,29,30]. We applied the photoabsorption cell/double-ion chamber method to characterize the intensity of light at 13.5 nm and to determine the AIOY values of the samples. The absolute photon intensity at 13.5 nm delivered from the LSGM beamline is essential information to derive AIOY from ionic outgassing, and was characterized on taking photoionization of argon as a reference. Using the photoabsorption cell and Lambert's law, we derived the photoabsorption cross-section of argon, $\sigma_{abs,Ar} = 1.39 \times 10^{-18}$ cm^2 (1.39 Mb), which agrees satisfactorily with 1.35 Mb reported by Samson and Stolte [20]. With the double-ion chamber, taking the absolute photoionization yield 1.065 [21], we derived the photon intensity as $3.0 \pm 0.6 \times 10^{12}$ photons s^{-1} between shifts in the same day as well as between experimental runs conducted months apart, under beamline conditions typical for this work: the entrance and exit slits of the LSGM beamline monochromator were typically open at 200 and 200 μm.

Fig. 1 shows the double-ion chamber setup of this study for the AIOY determination, as described briefly in the following. Two guard electrodes (length 1 cm) and two ion-collection electrodes (length 17 cm) were set at ground potential with respect to a bias +40 V applied to a cylindrical electrode. This cylindrical electrode collected electrons and repelled outgassed ions ejected from the sample. The ion-collection electrodes collected ions, from which the positive currents were recorded with two electrometers (Keithley, M617); the guard electrodes ensured an even electric field in the region of the double-ion-collection electrodes. Each sample for the AIOY measurement was taped on the tip of a sample holder, which was bolted to a push–pull longitudinal-motion vacuum component. The sample was positioned normal to the incident light, and the longitudinal axis of the cylindrical double-ion chamber coincided with the path of the EUV light and the push–pull axis of the sample. The taped sample was pushed from outside the double-ion chamber into it and underneath the second ion electrode for the ion collection. The efficiency of the ion collection was confirmed in two ways. Firstly, the ion current from ionic outgassing showed no observable position dependence within ±1% variation through a 9-cm push–pull travel distance underneath the second ion electrode. Secondly, a bias voltage increased from +40 to +120 V resulting in an increment <5% of the ion current. All AIOY values were determined on pushing the tested sample underneath the middle of the second ion-collection electrode. The first ion electrode collected spurious ions for the background measurement.

The outgassed ion current measured with the second ion-collection electrode was typically in a range 10^{-9} to 10^{-10} A, whereas the background current was of order 10^{-11} to 10^{-12} A. The vacuum conditions of the double-ion chamber, $\sim 1 \times 10^{-5}$ Pa, also ensured that outgassed ions reached the ion-collection electrode in a distance shorter than its mean free path. The EUV photon flux was 0.88 mJ cm^{-2} s^{-1} for an exposed area 0.5 × 0.1 cm^2 of the sample. The exposure area was examined on an overly exposed

sample with a profilometer (Veeco, Dektak 150); it was determined as the area enclosing the full width at half maximum of the ablated profile, and its uncertainty was estimated to be ±30%. The average outgassing ion current below an accumulated exposure dose <30 mJ cm^{-2} was converted into a number of charged particles per seconds; this number was then compared with the determined photon intensity; the AIOY value of a sample was thus determined as follows:

$$\text{AIOY} = \frac{i_2\,\text{C s}^{-1} \times N_A}{96,500\,\text{C mol}^{-1} \times \text{photon intensity}} \quad (1)$$

in which i_2 is the ion current through the second electrode after subtraction of the background, N_A is Avogadro's constant of charged particles per mole, one mole of singly charged particle is 96,500 C, and the photon intensity delivered from the beamline is typically ~3×10^{12} photons s^{-1}. The AIOY values of samples upon irradiation at 13.5 nm were verified at a fifth of that light intensity by closing the entrance and exit slits of the LSGM beamline to 50 μm × 100 μm; the equivalent photon intensity was then ~6×10^{11} photon s^{-1}. The photon flux (mJ cm^{-2} s^{-1}) is not a variable for deriving AIOY, and it is needed to know the exposure time needed for the AIOY data collection up to 30 mJ cm^{-2}.

2.2. Characterization of ionic outgassing

The experiment on ionic outgassing with the quadrupole mass filter (QMS, EXTREL, 150-QC) method has been described in detail elsewhere [18]. In the following text, we employ unit *u* instead of *u*/*z* for simplicity, as there is no indication of multiple-charged outgassing. Notably, the filament ionizer of QMS was not turned on in this study. Therefore, only direct ionic outgassing was measured instead of neutral outgassing, which must be ionized by the ionizer for the following QMS detection. We characterized outgassed ions qualitatively in the range 1–200 u; an observation of exposure decay of outgassed ions made impracticable a quantitative characterization in relation to beamtime. The decay of ionic outgassing is described in Section 3.3.

We measured the relative extent of CH_3^+, F^+, and $C_2H_5^+$ outgassing among samples by scanning through sample positions, a means that ensured measurement of fresh samples; the exposure dose was typically ~12 mJ cm^{-2} per measurement point. The relative extent of F^+ outgassing, which ion was observed as an important product, was derived in such a way that UL-1A served as the reference, and the other samples were taped between two reference samples for comparison of signals. The relative extents of CH_3^+ and $C_2H_5^+$ outgassing were derived in the same way.

When measuring ionic outgassing through the samples, we concurrently recorded the increase of steady-state pressure from each sample with an ion gauge (BA-type, Granville Philips). The exterior electric field of a pressure gauge of this type is expected to prevent ionic outgassing from reaching the collector electrode of the gauge; in this way the pressure rise was correlated with neutral outgassing from samples [18], and was measured relatively without application of gas correction factors [31]. The pressure rise was not of major interest in this work, but it provides additional information to elucidate the outgassing phenomena.

2.3. Chemical kinetics of EUV photochemistry leading to ionic outgassing

Ion intensities of F^+ and CH_3^+ (in some cases also of $C_2H_5^+$) were monitored with the QMS as a function of the exposure dose. First-order exposure kinetics was applied to derive the rate coefficient,

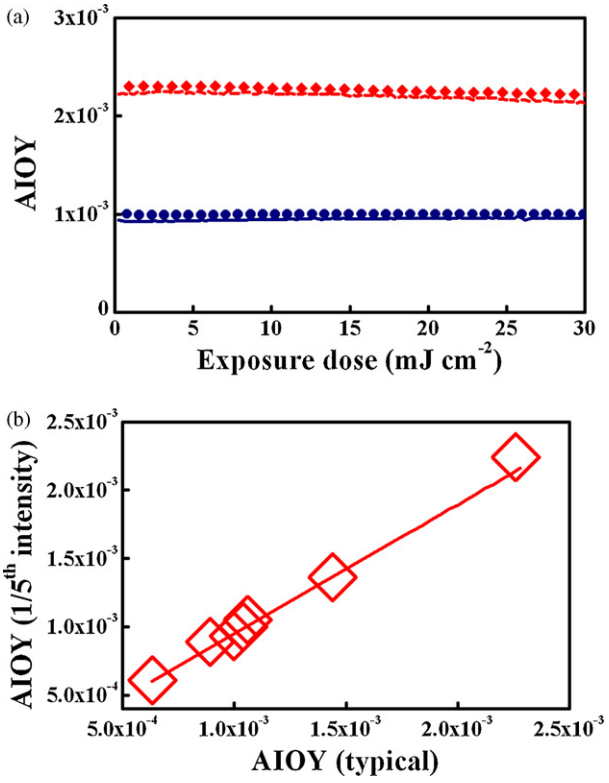

Fig. 2. (a) AIOY of RRR and UL-1A as a function of exposure dose. Under typical beamline conditions, RRR (●) and UL-1A (♦); decreased photon intensities, RRR (—) and UL-1A (—). (b) Consistency of AIOY values determined under typical beamline conditions and decreased photon intensities.

Dill's parameter C, for F^+ and CH_3^+ outgassing in the following way:

$$\ln\left(\frac{I_{\text{Ion},t}}{I_{\text{Ion},0}}\right) = -C_{\text{ion}} \times \text{photon flux} \times t = -C_{\text{ion}} \times \text{dose} \quad (2a)$$

$$d\,\ln\frac{\text{Ion intensity}}{d(\text{dose})} = -C_{\text{ion}} \quad (2b)$$

in which $I_{\text{Ion},0}$ and $I_{\text{Ion},t}$ are the intensities of ions CH_3^+ or F^+ at exposure times 0 and *t*, respectively; C_{ion} as C_{F^+} and $C_{CH_3^+}$ are the Dill's *C* parameters for reactions leading to outgassing of CH_3^+ or F^+, respectively. The decay of these intensities was conducted under typical beamline conditions and with the photon flux decreased to one quarter or one fifth of the typical values. The exposure rate coefficient was evaluated for an exposure dose typically <40 mJ cm^{-2}, for which the first-order photochemical reaction is a satisfactory approximation.

3. Results and discussion

Table 1 lists the results of ionic outgassing from PMMA, RRR, and twelve UL samples. The table includes the AIOY value, the relative extent of F^+, CH_3^+, and $C_2H_5^+$ outgassing, and the exposure rate constant as Dill's parameter *C* leading to F^+ and CH_3^+ outgassing.

3.1. Absolute ionic outgassing yield (AIOY)

Fig. 2(a) shows two typical AIOY measurements. The ion currents from ionic outgassing of RRR and UL-1A measured with the double-ion chamber method were converted to AIOY values according to Eq. (1) under the typical beamline conditions and decreased photon intensities. The AIOY value of each sample listed in Table 1 is an average value measured with exposure dose less than 30 mJ cm^{-2}, for which AIOY remains roughly constant. Fig. 2(b)

Table 1
Summary of ionic outgassing results.

Sample information		Photoresist		UL-polyester			UL-novolac			UL-PAG-attached-methacrylate			UL-methacrylate		
		PMMA	RRR	UL-1A	UL-1B	UL-1C	UL-2A	UL-2B	UL-2C	UL-3A	UL-3B	UL-3C	UL-4A	UL-4B	UL-4C
Absolute ionic outgassing yield (AIOY)		8.8×10^{-4}	9.7×10^{-4}	$2.2^5 \times 10^{-3}$	1.2×10^{-3}	$1.0^5 \times 10^{-3}$	8.8×10^{-4}	$1.1^5 \times 10^{-3}$	9.5×10^{-4}	$2.0^5 \times 10^{-3}$	1.15×10^{-3}	8.8×10^{-4}	6.2×10^{-4}	1.0×10^{-3}	1.1×10^{-3}
Relative extent of ionic outgassing	CH_3^+	4.01 ± 0.43	0.8 ± 0.4	1 ± 0.08	0.9 ± 0.1	1.2 ± 0.1	0.37 ±0.04	0.51 ± 0.05	0.75 ± 0.06	5.4 ± 0.5	4.0 ± 0.5	4.4 ± 0.4	0.25 ± 0.04	1.0 ± 0.1	1.0 ± 0.1
	$C_2H_5^+$	0.49 ± 0.06	2.9 ± 0.6	1 ± 0.10	2.9 ± 0.6	2.2 ± 0.4	0.57 ± 0.09	0.44 ± 0.07	1.1 ± 0.2	6.7 ± 1.0	6.0 ± 0.1	3.8 ± 0.5	3.1 ± 1.0	2.7 ± 0.4	2.2 ± 0.5
	F^+	0.02 ± 0.01	1.8 ± 0.4	1 ± 0.16	0.64 ± 0.12	1.0 ± 0.2	0.19 ± 0.03	0.66 ± 0.08	0.59 ± 0.08	11.2 ± 1.6	8.5 ± 1.1	7.9 ± 0.9	0.49 ± 0.08	0.24 ± 0.05	0.38 ± 0.07
Relative pressure rise		1	0.42	0.12	0.08	0.21	0	0	0.08	0.67	0.58	0.28	0.04	0.42	0.19
Double-bond equivalents per carbon atom			0.20	0.49	0.53	0.56	0.58	0.61	0.60	0.57	0.3	0.32	0.34	0.58	0.36	0.41
Rate constant (Dill's C parameter) for ionic outgassing in $cm^2\ mJ^{-1}$	$C_{CH_3^+}$	4.0×10^{-3}	6.1×10^{-3}	3.0×10^{-3}	4.0×10^{-3}	3.6×10^{-3}	1.8×10^{-3}			6.0×10^{-3}	6.1×10^{-3}	6.6×10^{-3}	2.7×10^{-3}	1.6×10^{-3}	2.1×10^{-3}
	C_{F^+}	–	1.1×10^{-2}	7.7×10^{-3}	–	6.9×10^{-3}	4.9×10^{-3}	5.8×10^{-3}	7.3×10^{-3}	7.0×10^{-3}	3.5×10^{-3}	3.9×10^{-3}	–	–	–

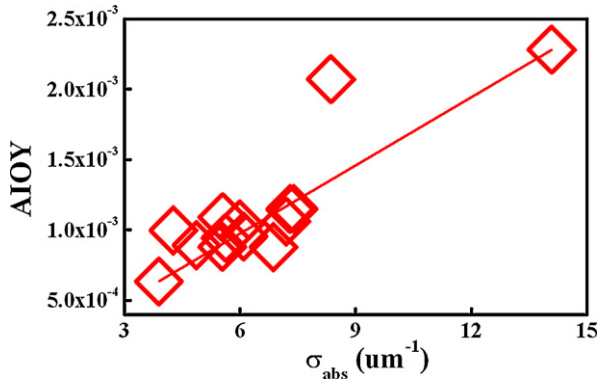

Fig. 3. Correlation between AIOY and σ_{abs} for PMMA, RRR, and twelve underlayer samples.

illustrates the consistency of the AIOY values determined under both beamline conditions for eight samples; a linear correlation with a value $R^2 = 0.99$ and a systematic difference <6% for values derived under two experimental conditions are obtained. This systematic difference represents the measurement precision of AIOY with the double-ion chamber method over a short period of shifts and two days, and is significantly less than the 20% uncertainty of absolute photon intensities determined from shifts, days and runs; the uncertainty of the AIOY values is thus considered to be ±20%.

The samples with large AIOY values are UL-1A, 2.3×10^{-3} and UL-3A, 2.2×10^{-3}; UL-1A was the only sample of this work that contained iodine to increase the effectiveness of EUV photoabsorption, whereas UL-3A is highly fluorinated. The AIOY values of other samples are all of order 10^{-3}, and show no dependence on film thickness: PMMA 125 nm, RRR 125 nm, and UL 30 nm. Furthermore, a satisfactory correlation exists between AIOY and the absorption coefficient (σ_{abs} in μm^{-1}) of the sample as shown in Fig. 3, in which α_{abs} of a sample was taken from an EUV reflectometry measurement [32]. As illustrated in Fig. 3, highly fluorinated UL-3A is the only sample of which the AIOY value deviates significantly from the linear correlation of AIOY with σ_{abs}; its exceptional AIOY value is discussed further in Section 3.2.

The lack of thin-film thickness dependence for ionic outgassing and a satisfactory correlation between AIOY and σ_{abs} values suggest a plausible photochemical mechanism that the ions can be photochemical products from direct dissociative photoionization that occurs on the surface. To estimate the depth at which ionic outgassing can occur, we assume that the quantum yield is approximated as unity for ionic outgassing at 13.5 nm, which is true for inert gases and numerous simple organic compounds [21], such as dimethyl ether and benzene [33,34]. With such an assumption, the AIOY value becomes proportional to $\sigma_{abs}D$; D is the escape depth of ions. The estimated escape depth of ions is then 0.17 ± 0.03 nm, an average value derived from fourteen samples, which is consistent in order of magnitude with a typical escape depth 0.3–0.4 nm for ions [35]. The assumption of ionic outgassing mainly from the surface is thus justified.

The equivalent ionic outgassing rate of RRR for an AIOY value of 9.7×10^{-4} is 2.6×10^{13} molecules s^{-1} cm^{-2} under an EUV power density at 0.4 W cm^{-2}, which is a scaled EUV flux for benchmarking resist outgassing [1]. In the latter case the outgassing rate was reported to range from 3.5×10^{13} to 7.8×10^{17} molecules s^{-1} cm^{-2} among eight institutes with three methods, presumably involving the detection of neutral species; the extent of that range implies that the quantum yields of neutral outgassing vary from 10^{-3} to 30. Can ionic and neutral outgassing be correlated, and what are the branching ratios of these two production channels? We examine these questions in the following sections.

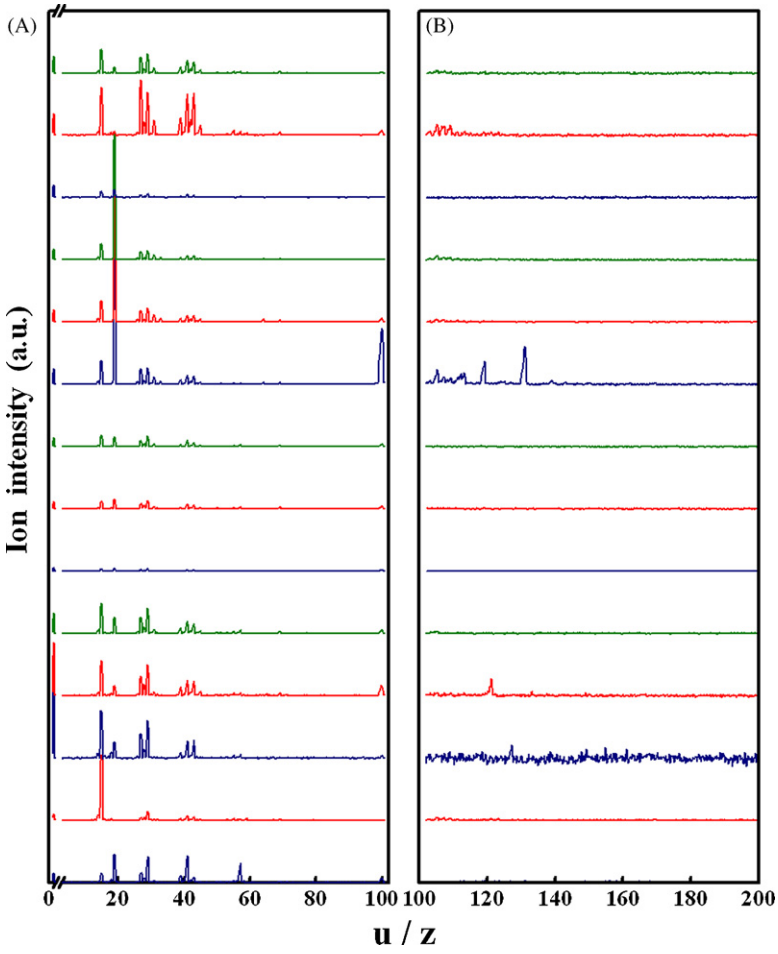

Fig. 4. Mass spectra of outgassed ions. Spectra are shifted by an additional unit for each successive sample. The spectra from bottom to top correspond to PMMA, RRR, UL-1A to 1C, UL-2A to -2C, UL-3A to -3C, and UL-4A to -4C. (a) 1–101 u, with 1 u (H^+) intensity demagnified to 1/10. (b) 101–200 u, with ion intensities magnified ten times.

3.2. Characterization of ionic outgassing

In addition to AIOY, the identities of outgassing ions are important for a further consideration of their potential damage to EUV optics. Fig. 4 shows mass spectra of the outgassed ions in the range 1–200 u from PMMA, RRR, and UL samples upon irradiation at 13.5 nm. The relative intensity of ions across the mass range is qualitative; the mass spectrum of each sample is nevertheless normalized at 15 u to its own relative extent of CH_3^+ outgassing, a quantity described later in this section.

For typical photoresist and UL materials containing hydrocarbons, fluorinated compositions or fluorine-containing photoacid generators, we identify common outgassed ions including H^+ at 1 u; F^+, CF^+, CF_2^+, and CF_3^+ (F^+ and $C_xF_y^+$) at 19, 31, 50, and 69 u, respectively; and CH_3^+, $C_2H_{3,5}^+$ and $C_3H_{3,5,7}^+$ ($C_nH_m^+$) at 15, 27, 29, 39, 41, and 43 u, respectively. $C_2F_4^+$ at 100 u has been identified previously in the PAG work as a characteristic species from the C_4F_9 moiety, and is observable from RRR of its PAG portion and most UL samples, which contain <0.5 mass% fluorinated additives. The importance of F^+ and $C_xF_y^+$ outgassing from fluorine-containing polymeric materials is thus indicated.

A unique ion CH_2F^+ at 33 u is identified from PAG-attached-methacrylates of UL-3A, -3B and -3C, but it is not observed from triflate or nonaflate of PAG [18], which contain no hydrogen within their perfluoroalkylsulfonate portions. UL-3A contains a perfluoroalkyl moiety C_8F_{17}, and emits additional and abundant outgassed ions $C_2F_5^+$ at 119 u and $C_3F_5^+$ at 131 u. The C_4H_9 moiety is a common side chain of a copolymer backbone and its PAG of RRR, $C_4H_9^+$ outgassing at 57 u, was an observable but weak species from PAG found in the previous work [18]; it is significant here from the dominant copolymer portion. Iodine is a major component of UL-1A but counted for only 0.9 mass% in RRR; outgassed I^+ at 127 u was observed from UL-1A and merely from RRR. Taking into account that the QMS detection efficiency deteriorates monotonically as a function of the ratio u/z, the I^+ outgassing from UL-1A is non-negligible. Mass peaks at 105, 107, 109, and 111 u were identified for UL-PAG-attached-methacrylates, UL-3A to -3C. The 105–111 features had been observed as major peaks from desorbed thiolate, C_6H_5S, in a photoionization study of self assembled monolayers [36]. The PAG portion of UL-PAG-attached-methacrylates can be unambiguously attributed to 105–111 u outgassing. We were not able to assign possible outgassing sources in two cases due to the lack of detailed chemical information: UL-1B at 121 u and UL-4B (containing no C_6H_5S according to NCI's information) at 105–111 u.

RRR contains ~95 mass% hydrocarbon, but the overall F^+ and $C_xF_y^+$ intensity is approximately one quarter of the overall ion intensity in the range 2–200 u. In contrast, in the previous work on RRR the side-chain cleavage leading to formation of isobutene and isobutane amounts to 90% of the outgassing from its *t*-butyl acrylate moiety [1]. PMMA liberates H^+ and $C_nH_m^+$ with no detectable production of carboxyl-containing ions, but previous reports showed that CO_2 at 44 u and $C_2H_4O_2$ at 60 u are important outgassed species [37,38]. The PMMA and RRR results clearly indicate that outgassed neutral and ion species can differ markedly; in an investigation of contamination one must examine outgassing of both types qualitatively and quantitatively.

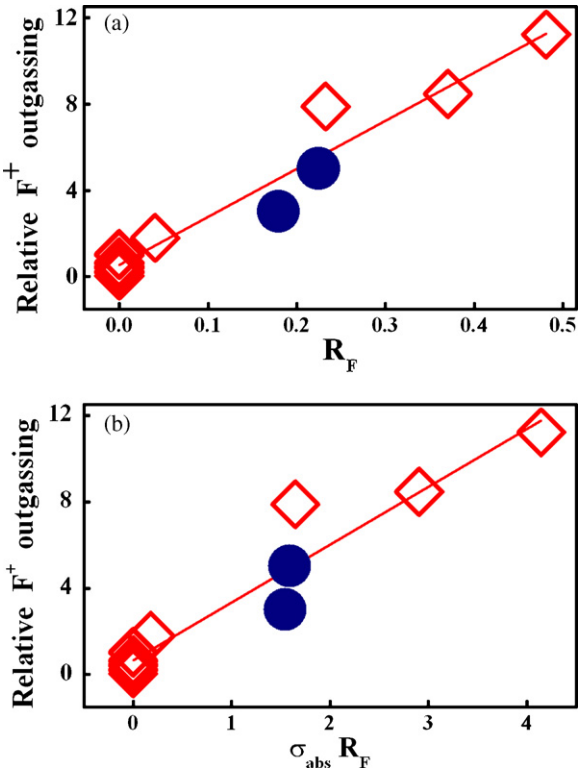

Fig. 5. Correlation between the relative extent of F^+ outgassing and (a) R_F, and (b) $\sigma_{abs} \times R_F$. (◊): fourteen samples and (●): other data.

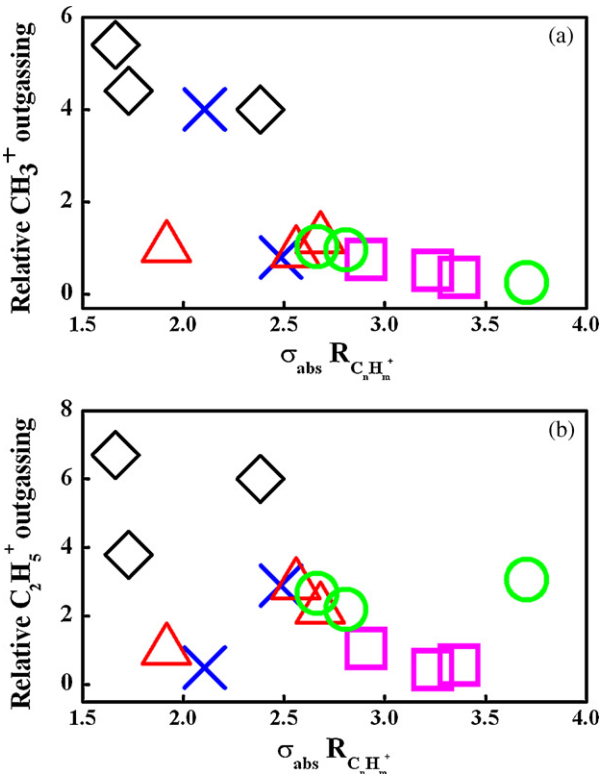

Fig. 6. Correlation between (a) CH_3^+ and (b) $C_2H_5^+$ outgassing and $\sigma_{abs} \times R_{C_nH_m}$. (×): photoresists, (△): UL-polyesters, (□): UL-novolac, (◊): UL-PAG-attached-methacrylate, and (○): methacrylate.

Our previous work on the ionic outgassing of PAG showed a satisfactory correlation between the extent of F^+ outgassing and the ratio of F photoabsorption to the overall photoabsorption (R_F) of the sample material; we argued there that the extent of F^+ outgassing is governed by F photoabsorption [18]. We tested this F-photoabsorption argument further in the present work, with R_F values obtained from

$$R_F = \frac{\text{fluorine photoabsorption}}{\text{overall photoabsorption}} = \frac{x_F \sigma_F}{\sum_i x_i \sigma_i} \quad (3)$$

in which x_F and x_i are the number fractions of F and element i within a sample, and σ_F and σ_i are atomic photoabsorption cross-sections at 13.5 nm for F and element i, respectively. The σ value of each element was obtained from information provided at the CXRO website [39].

Fig. 5(a) shows the extent of F^+ outgassing as a function of R_F for fourteen samples: the R_F values of only RRR, UL-3A, UL-3B, and 3C are significant; the R_F values of UL samples with fluorine-containing additives are intentionally set to zero, as they contain <0.5 mass% fluorinated additives with no information of chemical composition. PMMA, UL-1B, UL-4A to -4C are free of fluorine; their extents of F^+ outgassing are 0.36 ± 0.27, an average value that represents the level of measurement errors at 19 u. The figure includes values of two other UL samples, which were not targeted samples of this work but contain appropriate R_F values to make the correlation more evident. With $R^2 = 0.97$, a satisfactory correlation between the relative extent of F^+ outgassing and R_F is confirmed. According to reaction mechanisms for EUV photochemistry proposed in Section 3.3, the extent of F^+ outgassing is expect to be appropriately correlated with $\sigma_{abs} \times R_F$. Fig. 5(b) illustrates the F^+ outgassing $-\sigma_{abs} \times R_F$ correlation; again a correlation as satisfactory as that shown in Fig. 5(a) is obtained.

Fig. 6 depicts the correlation of CH_3^+ and $C_2H_5^+$ outgassing as a function of $\sigma_{abs} \times R_{C_nH_m}$, in which $R_{C_nH_m}$ of each sample is derived similarly to Eq. (3) from $(x_C\sigma_C + x_H\sigma_H)/\sum_i (x_i\sigma_i)$. No linear correlation between CH_3^+ or $C_2H_5^+$ outgassing and $\sigma_{abs} \times R_{C_nH_m}$ (or $R_{C_nH_m}$, not shown) is found, but some intriguing behaviors are observed in both figures. Firstly, PMMA and UL-PAG-attached-methacrylates (UL-3A to -3C), which contain a methylmethacrylate or methacrylate backbone, possess the least ratios of hydrocarbon photoabsorption, but they liberate CH_3^+ most abundantly in outgassing. Secondly, polyesters UL-1A to 1-C exhibit a similar extent of CH_3^+ outgassing, and likewise novolacs UL-2A to -2C and methacrylates UL-4A to -4C of CH_3^+ and $C_2H_5^+$ outgassing. UL-2A to -2C and UL-4A to -4C show a weak correlation between CH_3^+ outgassing and $\sigma_{abs} \times R_{C_nH_m}$. Thirdly, the overall trend of CH_3^+ and $C_2H_5^+$ outgassing is negatively dependent on the $\sigma_{abs} \times R_{C_nH_m}$ and $R_{C_nH_m}$ values.

These phenomena shown in Fig. 6 indicate that hydrocarbon outgassing depends on the polymer type. The key to a satisfactory correlation for CH_3^+ outgassing is to equate hydrocarbon proportions appropriately. Some polymer type might possess a greater proportion of aliphatic than aromatic composition, so liberating CH_3^+ and $C_2H_5^+$ outgassing to a greater extent without double-bond scission. We attempt to establish a relevant correlation from the above arguments, and obtain an improved correlation between CH_3^+ outgassing of the fourteen samples and their respective [σ_{abs}/(double-bond equivalent per carbon atom)] number, as shown in Fig. 7(a). The double-bond equivalent per carbon atom (BDEPC) is calculated with

$$\text{DBEPC} = \frac{2 \times N_C + 2 - N_{H/F}}{2N_C} \quad (4)$$

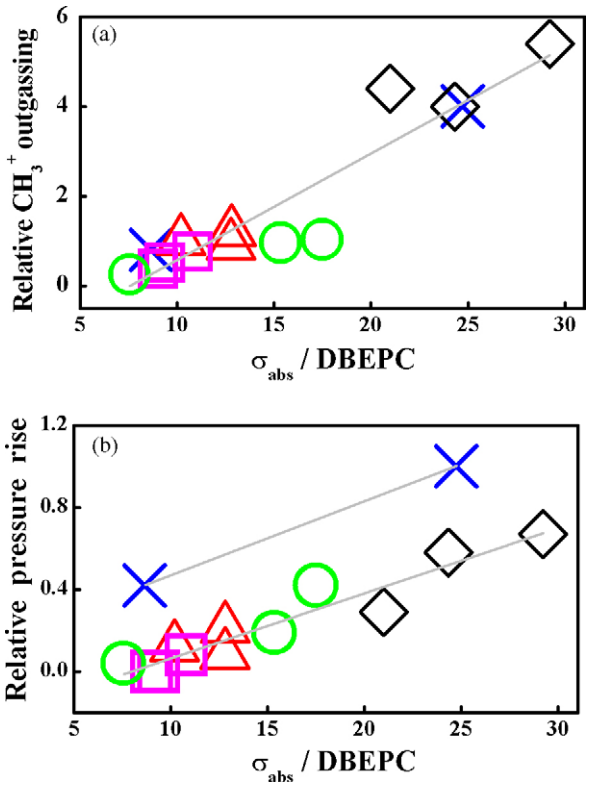

Fig. 7. (a) Correlation between CH_3^+ outgassing and σ_{abs}/DBEPC and (b) correlation between pressure rise and σ_{abs}/DBEPC. Same symbol definitions as in Fig. 6.

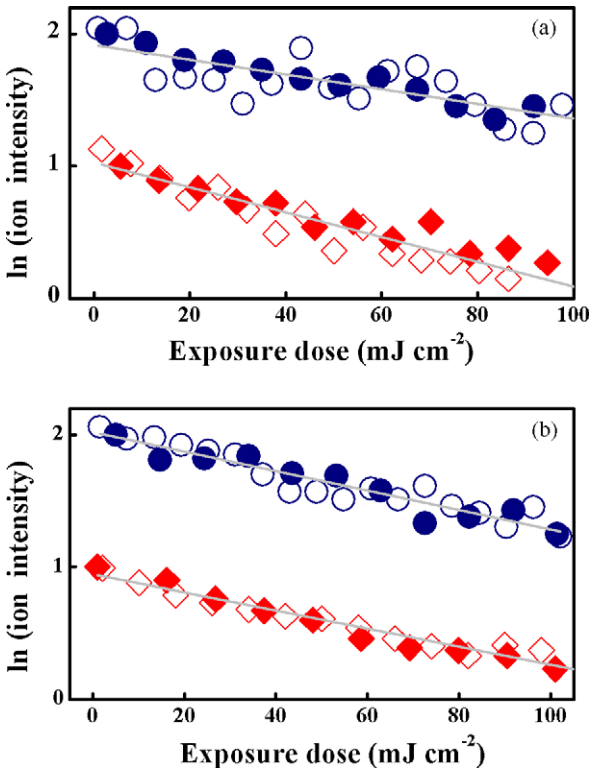

Fig. 8. Natural-logarithmic decays of F^+ and CH_3^+ outgassing (I_{ion}) of (a) RRR and (b) UL-3A, as a function of exposure dose. Under typical beamline conditions for CH_3^+ (●) and F^+ (♦), and at a fifth of the photon flux for CH_3^+ (○) and F^+ (◊).

in which N_C and $N_{H/F}$ are the numbers of carbon and (hydrogen + fluorine) atoms of the molecular formula of the sample, respectively. The DBEPC number defines the effective multiple-bonding characteristic of an average carbon atom. As the formulae of the fourteen samples are confidential, only the resulting values are shown in Fig. 7. Notably, the σ_{abs} value of UL-1A does not include iodine photoabsorption, which accounts for >50% of its EUV photoabsorption and liberates I^+ outgassing as shown in Fig. 4. The DBE and Ohnishi numbers are two common metrics for estimating the etch resistance of photoresists [40], and they represent the alkyl or aryl nature of the sample; the greater is the DBEPC number and the smaller is the Ohnishi number, the greater is the aryl nature of the sample. The Onishi number had been used analogously to correlate outgassing of four EUV model resists [41], but we found no correlation between CH_3^+ outgassing and the Ohnishi number.

A correlation between the structural metric DBEPC of polymers and neutral outgassing is also found. Fig. 7(b) illustrates the pressure rise from fourteen samples of different polymer types, and shows again a linear correlation with σ_{abs}/BDEPC. Furthermore, the pressure rise clearly separates into two groups, photoresists and UL samples: the amount of pressure rise from photoresists has a slope similar to that from UL samples but is shifted to greater values. This figure reveals that the pressure rise depends on thickness. For the pressure rise representing the extent of neutral outgassing, as this study posits, the thin-film thickness dependency for neutral outgassing makes the same hypothesis as that proposed previously, but based on the results of two samples [25]. Other authors suggested the mitigation of outgassing on adding aromatic structure to the resist design [37,41,42]; in Fig. 7 we show here quantitatively that the $C_nH_m^+$ outgassing and pressure rise are linearly correlated with the σ_{abs}/DBEPC structural metric.

Among samples measured as shown in Figs. 5 and 7 and listed in Table 1, the UL-novolacs samples are the most stable underlayer material being evaluated, whereas the PMMA and UL-PAG-attached-methacrylate are highly reactive upon irradiation at 13.5 nm, and UL-3A is the least stable. The AOIY of each sample includes F^+ outgassing dependent on $\sigma_{abs} \times R_F$, CH_3^+ (and $C_nH_m^+$) outgassing dependent on polymer type and more specifically on σ_{abs}/DBEPC; in summary of the AOIY value, H^+ outgassing or other ionic outgassing not examined here might be important to bestow consistency among AIOY, F^+, and $C_nH_m^+$ values. For example, UL-1A has the greatest AIOY value but a moderate extent of F^+ and $C_nH_m^+$ outgassing; although only a qualitative conclusion can be drawn according to Fig. 4, H^+ outgassing of UL-1A is more than five times that of most samples, and it also liberates non-negligible I^+ in the outgassing; both H^+ and I^+ outgassing can be part of its high AIOY value. In contrast, the unexpectedly large AIOY value of UL-3A illustrated in Fig. 3 remains for discussion. The H^+ outgassing of UL-3A to -3C is similar to that of other samples, and its F^+ and CH_3^+ outgassing conform to the $\sigma_{abs} \times R_F$ and $\sigma_{abs} \times$ DBEPC predictions. The dissimilarity of UL-3A from the other samples is that the photoabsorption by the perfluoroalkyl portion of the sample amounts to >60% of its overall photoabsorption. Breakage of a single bond in a given polymeric resin might not produce outgassing, but each bond breakage of the long-chain C_8F_{17} moiety of UL-3A can immediately liberate $C_xF_y^+$ in outgassing. Fig. 4 shows that $C_2F_4^+$ outgassing is important when taking the QMS detection efficiency into account, and $C_2F_4^+$ outgassing can be the major contribution to the unexpectedly large AIOY value of UL-3A.

3.3. First-order exposure kinetics for ionic outgassing

While measuring the relative extent of F^+ outgassing, we observed a significant decay of F^+ outgassing as a function of the accumulated dose. Fig. 8(a) and (b) shows natural-logarithmic decays of F^+ and CH_3^+ outgassing as a function of the exposure dose <30 mJ/cm^{-2} for RRR and UL-3A, respectively. Fig. 7(a) and (b) includes measurements under typical beamline conditions and a

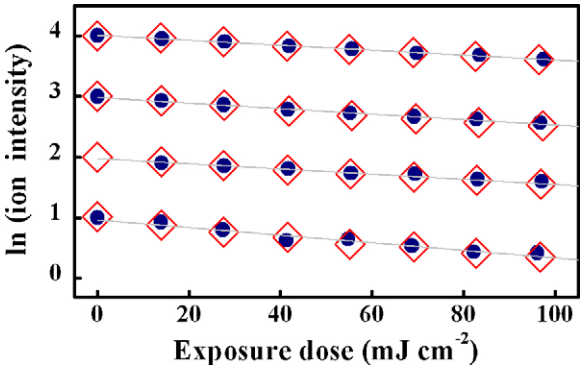

Fig. 9. Natural-logarithmic decays of CH_3^+ and $C_2H_5^+$ outgassing as a function of exposure dose. The decay curves from bottom to up are for RRR, UL-3A, UL-3B, and UL-3C, respectively with a shift of one unit for each successive sample. (●): CH_3^+ and (◊): $C_2H_5^+$.

fifth of the photon flux. Table 1 lists the resulting first-order exposure rate coefficients C_{F^+} and $C_{CH_3^+}$ of the fourteen samples derived according to Eq. (2). The experimental uncertainty of Dill's *C* values listed in Table 1 is typically ≤±40%. R^2 of the linear fit to Eq. (2) is invariably >0.9 and generally >0.97, which demonstrates a minor contribution to the experimental uncertainty. The photon flux is the major source of uncertainty; it contains the uncertainties of the photon intensity, 20%, and the definition of the exposed area, ≤35%.

The resulting values of C_{F^+} and $C_{CH_3^+}$ listed in Table 1 indicate EUV photochemical behaviors described as follows:

(A) $C_{F^+} \neq C_{CH_3^+}$. $C_{F+} > C_{CH_3^+}$ is obtained for most samples, and $C_{F+} \leq C_{CH_3^+}$ for the UL-PAG-attached-methacrylate samples.

(B) The $C_{CH_3^+}$ values for the same polymer type are similar within experimental uncertainty. Examples include $3.0–3.6 \times 10^{-3}$, $6.0–6.6 \times 10^{-3}$, and $1.6–2.7 \times 10^{-3}$ mJ^{-1} cm^2 for UL-polyesters, UL-PAG-attached-methacrylates, and UL-methacrylate, respectively. (The rate coefficients of UL-novolacs leading to CH_3^+ outgassing are among the smallest; only $C_{CH_3^+}$ of UL-2A was measured.) Furthermore, Dill's C parameters pertaining to CH_3^+ and $C_2H_5^+$ outgassing are the same within experimental uncertainty for the few samples measured. Fig. 9 depicts the natural-logarithmic decays of CH_3^+ and $C_2H_5^+$ outgassing from PMMA, RRR, and UL-PAG-attached-methacrylates as a function of exposure dose. The outgassed CH_3^+ and $C_2H_5^+$ fragments presumably emanate from the *t*-butyl portion, MMA unit and MA unit of the corresponding sample.

(C) The C_{F^+} values of the same fluorine-containing compositions are similar within the experimental uncertainty, even when the fluorine-containing portions are added to polymers of other types. UL-polyester and UL-novolac samples contain the same fluorine-containing additives, <0.5 mass%, and the derived C_{F^+} values are similar in the range 0.0049 ± 0.0015 to 0.0077 ± 0.0017 mJ^{-1} cm^2. In contrast, another PAG moiety shows an altered rate of depletion for F^+ outgassing. The C_{F^+} values are RRR (0.011 ± 0.0035), UL-3A (0.0070 ± 0.0017), UL-3B (0.0035 ± 0.0008) and UL-3C (0.0039 ± 0.0008) mJ^{-1} cm^2; the exposure rate of a factor two among them is experimentally significant. The lengths of carbon chains of the perfluoroalkylsulfonate moiety for RRR and the average length for UL-PAG-attached-methacrylates are in the order RRR ~ UL-3A > UL-3B > UL-3C. The longer is the perfluoroalkyl carbon chain, the greater is the rate of reaction.

We suggest that $C_{F^+} \neq C_{CH_3^+}$; the $C_{CH_3^+}$ values are similar for the same polymer type, and the C_{F^+} values for the same fluorine-containing compositions are similar. The UL-methacrylate samples (UL-4A to -4C) are remarkable: the DBEPC values varies from 0.36 to 0.58, which is a significant modification of their bonding characteristics, but the portion leading to CH_3^+ outgassing from each sample behaves similarly. These results hint that the kinetics of EUV exposure can differ from those of DUV, which have been used to describe DUV exposure. The reaction mechanisms of DUV photochemistry include a photoexcitation-deactivation pre-equilibrium reaction followed by a reaction generating photoacid [43]. DUV light excites a particular valence state mainly at the PAG site; the excitation efficiency can thus vary significantly when the same PAG alters its formulation from blended to attached to the polymeric structure [44]. An EUV excitation involves the excitation of an electron from a core level of an atom in the sample with little concern for the valence state. A reaction mechanism for EUV photochemistry is thus proposed to account for the ionic outgassing and pressure rise behavior observed in this work. The reaction mechanisms are analogous to DUV, but take the atomic or moiety contribution into account as follows:

$$M_j \xrightarrow{k_{j,1}} M_j^* \quad (5a)$$

$$M_j^* \xrightarrow{k_{j,-1}} M_j \quad (5b)$$

$$M_j^* \xrightarrow{k_{j,2}^+} P_j^+ \quad (5c)$$

$$M_j^* \xrightarrow{k_{j,2}^{neutral}} P_j \quad (5d)$$

in which at any given exposure duration *t*, M_j is a reactive '*j*' moiety containing particular atomic elements or a moiety within the sample; M_j^* denotes the photoactivated transient species of '*j*'; P_j^+ refers to the outgassed ion; and P_j represents the neutral fragment. M_j is PAG or a fluorinated additive within the samples leading to F^+ outgassing, whereas it is a particular portion within a polymer producing $C_nH_m^+$ outgassing. The rate coefficients $k_{j,1}$, $k_{j,-1}$, and $(k_{j,2}^+ + k_{j,2}^{neutral})$ refer to the forward excitation reaction by photoabsorption, the reverse deactivation reactions, and the product formation of ionic P_j^+ and neutral P_j, respectively. Applying the steady-state approximation to $[M_j^*]$, we obtain a rate equation of the product formation:

$$-\frac{d[M_j]}{dt} = \frac{d([P_j^+] + [P_j])}{dt} = k_{j,2}[M_j^*] = \frac{k_{j,1}k_{j,2}[M_j]}{(k_{j,-1} + k_{j,2})} \quad (6a)$$

$$[M_j] = [M_j]_0 e^{-[(k_{j,1}k_{j,2})/(k_{j,-1}+k_{j,2})]t} \quad (6b)$$

in which $[M_j]_0$ is the initial concentration of the reactive species on the surface producing outgassing, and $k_{2,j} = (k_{j,2}^+ + k_{j,2}^{neutral})$. For the ionic outgassing experiment, the observed intensities of CH_3^+ and F^+ are proportional to the instantaneous rate of ion formation; thus,

$$\text{Ion intensity} \propto \frac{d[P_j^+]}{dt} = \frac{k_{j,1}k_{j,2}^+[M_j]_0 e^{-[(k_{j,1}k_{j,2})/(k_{j,-1}+k_{j,2})]t}}{k_{j,1} + k_{j,2}} \quad (7a)$$

$$\frac{d\ \ln(\text{ion intensity})}{dt} = -\frac{k_{j,1}k_{j,2}}{k_{j,1} + k_{j,2}} \quad (7b)$$

Eq. (7b) can be reformulated to the standard equation for the exposure rate, and then combined with Eq. (6a) to obtain

$$\frac{d\ \ln(\text{ion intensity})}{d(\text{dose})} = \frac{d\ \ln([M_j]}{d(\text{dose})} = -\frac{(k_{j,1}/\text{photon flux})k_{j,2}}{(k_{j,1} + k_{j,2})} = -C_j \quad (8)$$

The derived Dill *C* parameter is proportional to the rate of EUV photoexcitation and a partition factor of the rate of product formation over the overall deactivation rates, i.e. the quantum yield

for overall outgassing; it does not depend on the concentration of the reactive compositions. Eq. (8) thus explains the observation $C_{F^+} \neq C_{CH_3^+}$, as F^+ and CH_3^+ are products of separate '*j*' moieties within a sample. The implication of Eq. (8) supports an observation that various samples of a same polymeric type have a similar $C_{CH_3^+}$ value, so the same fluorinated additives added to various samples show a similar C_{F^+} value.

The correlation between the relative extent of F^+ outgassing and $\sigma_{abs}R_F$ as shown in Fig. 5 is also explicable with Eq. (7a), which predicts the relative F^+ outgassing among fresh samples ($t \sim 0$) depends on $k_{j,1}k_{j,2}^{+}[M_j]_0/(k_{j,1}+k_{j,2})$. This quantity is further decomposable into the quantum yield (Φ) of the reaction, $\Phi = k_{j,2}^{+}/(k_{j,1}+k_{j,2})$, and the F photoabsorption, $k_{j,1}[M_j]_0 = \sigma_F[F]_0 = \sigma_{abs}R_F$. We reasonably assume that $k_{j,1}$, $k_{j,-1}$, and $k_{j,2}^{+}$ values are constant for EUV photochemical reactions of F-containing portions in separate samples, and $k_{j,2}^{neutral}$ is negligible for the reason that most neutral outgassing experiments showed no F-containing outgassing or its presence as a minor product. According to the above arguments, the quantum yield of F^+ outgassing is constant, and the relative extent of F^+ outgassing is then simply proportional $\sigma_{abs} \times R_F$.

A valid relation between not only CH_3^+ outgassing but also the pressure rise and σ_{abs}/DBEPC in Fig. 7(a) and (b) is qualitatively elucidated as follows. The product CH_3^+ (and C_nH_{m+} with the same Dill C as shown in Fig. 9) and neutral outgassing are likely generated in a concerted way; outgassing of both kinds described with Eqs. (5c) and (5d) then results from one reaction path, $M_j^* \xrightarrow{k_{j,2}} P_j^+ + P_j$; and Eq. (7a) becomes reformulated as follows:

$$\text{Pressure rise} \propto \frac{d[P_j]}{dt} = \frac{k_{j,1}k_{j,2}[M_j]_0}{(k_{j,1}+k_{j,2})} \qquad (7a')$$

The quantum yield (Φ) is implied to be the same, and is $\Phi = k_{j,2}/(k_{j,1}+k_{j,2})$ for a polymer of a given type that contains a particular hydrocarbon moiety to liberate $C_nH_m^+$ and neutral outgassing. The extent of $C_nH_m^+$ and neutral outgassing from a fresh sample thus depends on $k_{j,1}[M_j]_0$ among samples of the same polymer type; the polymeric samples contain mainly hydrocarbons, and $k_{j,1}$ is thus proportional to the overall σ_{abs}; the BDEPC value is an metric inversely proportional to the relative amount of $[M_j]_0$. For polymers of various types the DBEPC parameter serves as the metric to predict the polymer's lability, thus affecting $k_{j,-1}$ and $k_{j,2}$ and the quantum yield to $C_nH_m^+$ and neutral outgassing.

The only comparable Dill *C* value is the rate coefficient for the acid generation of RRR, reported as $0.144\,mJ^{-1}\,cm^2$ by a base "standard addition" method [45]. We derived $0.011 \pm 0.0035\,mJ^{-1}\,cm^2$ and $0.0061 \pm 0.0027\,mJ^{-1}\,cm^2$ for RRR upon irradiation at 13.5 nm leading to F^+ and CH_3^+ outgassing, respectively. The AIOY value of RRR varied insignificantly for an accumulated dose up to $30\,mJ\,cm^{-2}$ as shown in Fig. 2(a), and a preliminary measurement of the rate coefficient for H^+ outgassing indicates that its value is smaller than that of CH_3^+; both rate constants are thus expected to be smaller than C_{F^+} and $C_{CH_3^+}$. We measured directly the depletion of reactive species, and there is no experimental evidence to indicate that our Dill *C* parameter is underestimated. The rate coefficient for the formation of photoacids by EUV light involves reactions of photoionization within the polymer matrix as the first photochemical event, and subsequent reactions by secondary electrons; furthermore, the standard addition method to derive the Dill *C* parameter measured the dose to clear E_0 of tested films after post-exposure baking (PEB) for resists containing known and varied amounts of base quenchers [46]. Greater than ten times the difference in the Dill C parameter between the directly measured ionic outgassing reactions in this work and multiple steps for photoacid formation in previous work might be ascribed partly to an additional gain by reactions of secondary electrons [26], or catalytic gain of photoacid before the acid–base quencher neutralization; this effect is expected to be present but has not been addressed by the standard addition method.

4. Conclusion

We here report the first measurement of the absolute ionic outgassing yield (AIOY) for the PMMA, round-robin resist, and twelve underlayer materials. The AIOY values for these samples are all of order 10^{-3}, which means their rate of ionic outgassing is of order 10^{13} molecules $cm^{-2}\,s^{-1}$ @ $0.4\,W\,cm^{-2}$, and is 2.6×10^{13} molecules $s^{-1}\,cm^{-2}$ for the round-robin resist. The linear correlation between AIOY and absorption coefficient (σ_{abs}) of samples with no dependence on film thickness indicates that ionic outgassing occurs on the surface; the derived escape depth for ions is 0.17 ± 0.03 nm, a result consistent with a sub-nm escape depth for ions [35].

H^+, F^+, $C_xF_y^+$, and $C_nH_m^+$ outgassing are characterized as major outgassed ions from fourteen tested samples; other characterization results include CFH_2^+ from UL-PAG-attached-methacrylate samples, $C_4H_9^+$ outgassing from the *t*-C_4H_9 moiety, and I^+ outgassing from iodine-containing compounds. This work and previous PAG work demonstrate unambiguously that F^+ outgassing is important and directly correlated with the ratio of fluorine photoabsorption in the overall photoabsorption of the sample (R_F and $\sigma_{abs}R_F$). This F^+ outgassing study and new evidence of F-contamination on EUV optics [25] raise concern of the worsening contamination caused by the increment of fluorination in order to enhance the resist sensitivity [17,27,28]. The relative extents of CH_3^+ ($C_2H_5^+$) outgassing and pressure rise depend on the polymer type, and their values correlate well with a new metric defined here as (σ_{abs}/DBEPC); the double-bond equivalent per carbon atom indicates the lability of the sample to liberate $C_nH_m^+$ outgassing. A highly fluorinated sample UL-3A emits the most abundant amount of F^+ and $C_nH_m^+$ outgassing, and a comparable amount of $C_2F_4^+$ from its C_8F_{17} moiety; the additional $C_2F_4^+$ outgassing results in AIOY value being larger than expected.

We determined the rate coefficient for EUV photochemical reactions generating F^+ and CH_3^+ ($C_2H_5^+$) outgassing, and conclude as follows: $C_{F^+} \neq C_{CH_3^+}$, $C_{CH_3^+}$ values for the same polymer type are similar, and C_{F^+} values for the same fluorine-containing compositions are similar. Reaction mechanisms for EUV photochemistry are proposed to elucidate most results of this work. The Dill parameters C_{F^+} and $C_{CH_3^+}$ of the round-robin resist are 0.011 ± 0.0035 and $0.0061 \pm 0.0027\,mJ^{-1}\,cm^2$, respectively. Both values are less than a tenth of $0.144\,mJ^{-1}\,cm^2$ determined by a base standard addition method [45]; the discrepancy might arise from additional reactions due to secondary electrons or an additional catalytic gain of photoacid before the acid–base quencher neutralization in previous work.

Acknowledgements

National Science Council (NSC) of the Republic of China supports this work under contract NSC 98-2120-M-009-007 and NSC98-2113-M-390-005. The photoresists and underlayer materials are provided by Nissan Chemical Industries, Ltd. (NCI). The authors would like to thank R. Sakamoto-San, T. Endo-San, and Dr. Bang-C. Ho of NCI for useful discussions. We are grateful to Dr. Bing-Ming Cheng of National Synchrotron Radiation Research Center for loaning us the QMS apparatus.

References

[1] K.R. Dean, I. Nishiyama, H. Oizumi, A. Keen, H. Cao, W. Yueh, T. Watanabe, P. Lacovig, L. Rumiz, G. Denbeaux, J. Simon, An analysis of EUV resist outgassing measurements, Proc. SPIE 6519 (2007), 65191P-1-7.

[2] S. Kobayashi, J.J. Santillan, T. Itani, EUV resist outgassing: quantification and release mechanisms, J. Photopolym. Sci. Technol. 21 (2008) 469–474.
[3] J.J. Santillan, S. Kobayashi, T. Itani, Outgassing quantification analysis of extreme ultraviolet resists, Jpn. J. Appl. Phys. 47 (2008) 4922–4925.
[4] S. Kobayashi, J.J. Santillan, H. Oizumi, T. Itani, EUV resist outgassing quantification and application, Proc. SPIE 7273 (2009), 72731P-1-12.
[5] S. Kobayashi, J.J. Santillan, H. Oizumi, T. Itani, EUV resist outgassing release characterization and analysis, Microelectron. Eng. 86 (2009) 479–482.
[6] S.B. Hill, N.S. Faradzhev, C.S. Tarrio, T.B. Lucatorto, R.A. Bartynski, B.V. Yakshinskiy, T.E. Madey, Measuring the EUV-induced contamination rates of TiO_2-capped multilayer optics by anticipated production-environment hydrocarbons, Proc. SPIE 7271 (2009), 727113-1-11.
[7] N. Harned, R. Moors, M. van Kampen, V. Banine, J. Huijbregtse, R. Vanneer, A. Kempen, D. Ehm, R. Verberk, E. te Sligte, A. Storm, Strategy for minimizing EUV optics contamination during exposure, 2008, in: International Symposium on Extreme Ultraviolet Lithography, Lake Tahoe/CA, October, 2008.
[8] K. Orvek, G. Denbeaux, A. Antohe, R. Garg, C. Mbanaso, EUVL optics contamination from resist outgassing; status overview, 2008, in: International Symposium on Extreme Ultraviolet Lithography, Lake Tahoe/CA, October, 2008.
[9] K.R. Kim, K.E. Gonsalves, M. Thiyagarajan, Effects of material design on extreme ultraviolet (EUV) resist outgassing, Proc. SPIE 6153 (2006), 61531E-1-9.
[10] K.R. Dean, G. Denbeaux, A. Wüest, R. Garg, EUV resist outgassing: how much is too much? J. Photopolym. Sci. Technol. 20 (2007) 393–402.
[11] The 2007 Edition of the *ITRS*: Lithography, 2007 International Technology Roadmap for Semiconductor: http://www.itrs.net/Links/2007ITRS/Home2007.htm.
[12] V. Thirumala, H. Cao, W. Yueh, H. Choi, V. Golovkina, J. Wallace, P. Nealey, D. Thielman, F. Cerrina, Characterization of outgassing for EUV technology, Proc. SPIE 5376 (2004) 765–772.
[13] W. Yueh, H.B. Cao, V. Thirumala, H. Choi, Quantification of EUV resist outgassing, Proc. SPIE 5753 (2005) 765–770.
[14] A.O. Antohe, C. Mbanaso, Y.-J. Fan, L. Yankulin, R. Garg, P. Thomas, G. Denbeaux, E.C. Piscani, A.F. Wuest, EUV resist outgassing–scaling to HVM intensity, Proc. SPIE 7271 (2009), 727126-1-7.
[15] M.M. Chauhan, P.F. Nealey, Outgassing of photoresists in extreme ultraviolet lithography, J. Vac. Sci. Technol. B 18 (2000) 3402–3407.
[16] T. Watanabe, H. Hada, S.Y. Lee, H. Kinoshita, K. Hamamoto, H. Komano, Development of fast-photospeed chemically amplified resist in extreme ultraviolet lithography, Jpn. J. Appl. Phys. 44 (2005) 5866–5870.
[17] T. Sasaki, O. Yokokoji, T. Watanabe, H. Kinoshita, Development of partially fluorinated EUV-resist polymers for LER and sensitivity improvement, Proc. SPIE 6923 (2008), 692347-1-7.
[18] G.H. Ho, C.-J. Liu, C.-H. Yen, M.-H. Ho, S.-Y. Wu, Ionic outgassing from photoacid generators upon irradiation at 13.5 nm, Microelectron. Eng. 85 (2008) 2213–2219.
[19] J.W. Gallagher, C.E. Brion, J.A.R. Samson, P.W. Langhoff, Absolute cross sections for molecular photoabsorption, partial photoionization, and ionic photofragmentation processes, J. Phys. Chem. Ref. Data 17 (1998) 9–153.
[20] J.A.R. Samson, W.C. Stolte, Precision measurements of the total photoionization cross sections of He, Ne, Ar, Kr, and Xe, J. Electron Spectrosc. Relat. Phenom. 123 (2002) 265–276.
[21] A. Kobayashi, G. Fujiki, A. Okaji, T. Masuoka, Ionization cross section of rare-gas atoms (Ne, Ar, Kr and Xe) by electron impact from threshold to 1 keV, J. Phys. B 35 (2002) 2087–2103.
[22] C.A. Mayhew, D. Smith, The reactions of F^+ ions at thermal energies, J. Phys. B 23 (1990) 3139–3146.
[23] L.W. Sieck, S.G. Lias, Rate coefficients for ion-molecule reactions. I. Ions containing C and H, J. Phys. Chem. Ref. Data 5 (1976) 1123–1146.
[24] M.A. Lieberman, A.J. Lichtenberg, Principle of Plasma Discharges and Materials Processing, John Wiley, New York, 1994.
[25] I. Pollentier, G. Aksenov, A.-M. Goethals, R. Gronheid, R. Jonckheere, M. Leeson, Measurement and analysis of EUV photoresist related outgassing and contamination, Proc. SPIE 7271 (2009), 727146-1-9.
[26] H. Yamamoto, T. Kozawa, S. Tagawa, H. Yukawa, M. Sato, J. Onodera, Enhancement of acid production in chemically amplified resist for extreme ultraviolet lithography, Appl. Phys. Express. 1 (2008), 047001-1-3.
[27] R. Brainard, G. Higgins, E. Hassanein, R. Matyi, A. Wüest, Film quantum yields of ultrahigh PAG EUV photoresists, J. Photopolym. Sci. Technol. 21 (2008) 457–465.
[28] M. Wang, C.-T. Lee, C.L. Henderson, W. Yueh, J.M. Roberts, K.F. Gonsalves, Synthesis and properties of new anionic photoacid generators bound polymer resists for e-beam and EUV lithography, Proc. SPIE 6923 (2008), 692312-1-7.
[29] G.H. Ho, Absolute photoabsorption cross section of CCl_4 in the energy range 6–250 eV, Chem. Phys. 226 (1998) 101–111.
[30] G.H. Ho, M.S. Lin, Y.L. Wang, T.W. Chang, Photoabsorption and photoionization of propyne, J. Chem. Phys. 109 (1998) 5868–5879.
[31] J.F. O'Hanlon, A User's Guide to Vacuum Technology, 3r ed., John Wiley, New Jersey, 2003.
[32] G.H. Ho, F.-H. Kang, Y.-H. Shih, H.-S. Fung, H.-W. Fu, R. Sakamoto, T. Endo, B.-C. Ho, Y.-T. Huang, B.-Y. Shew, EUV reflectometry for determining the optical properties of photoresists and underlayer materials upon irradiation at 13.5-nm, 2009, in: International Workshop on EUV Lithography, Oahu, Hawaii, July, 2009.
[33] R. Feng, G. Cooper, C.E. Brion, Ionic photofragmentation and photoionization of dimethyl ether in the VUV and soft X-ray regions (8.5–80 eV)—absolute oscillator strengths for molecular and dissociative photoionization, Chem. Phys. 270 (2001) 319–332.
[34] R. Feng, G. Cooper, C.E. Brion, Dipole (e, e+ion) spectroscopic studies of benzene: absolute oscillator strengths for molecular and dissociative photoionization in the VUV and soft X-ray regions, J. Electron. Spectrosc. Relat. Phenom. 123 (2002) 211–223.
[35] S. Hofmann, Ultimate depth resolution and profile reconstruction in sputter profiling with AES and SIMS, Surf. Interface Anal. 30 (2000) 228–236.
[36] B.V. King, M.R. Savina, C.E. Tripa, W.F. Calaway, I.V. Veryovkin, J.F. Moore, M.J. Pellin, Single photon ionization of self assembled monolayers, Nucl. Instr. Meth. Phys. Res. B 190 (2002) 203–206.
[37] P.M. Dentinger, Outgassing of photoresist materials at extreme ultraviolet wavelengths, J. Vac. Sci. Technol. B 18 (2000) 3364–3370.
[38] G. Denbeaux, R. Garg, J. Waterman, C. Mbanaso, J. Netten, R. Brainard, Y.-J. Fan, L. Yankulin, A. Antohe, K. DeMarco, M. Jaffe, M. Waldron, K. Dean, Quantitative measurement of EUV resist outgassing, Proc. SPIE 6533 (2007), 653318-1-5.
[39] Center for X-ray optics (CXRO) at Berkeley National Laboratory website, http://henke.lbl.gov/optical_constants/.
[40] R.R. Dammel, New development in high-performance resist materials, J. Photopolym. Sci. Technol. 11 (1998) 687–704.
[41] H. Hada, T. Hirayama, D. Shiono, J. Onodera, T. Watanabe, S.Y. Lee, H. Kinoshita, Outgassing characteristics of low-molecular-weight resists for extreme ultraviolet lithography, Jpn. J. Appl. Phys. 44 (2005) 5824–5828.
[42] D.J. Guerrero, C. Beaman, R. Sakamoto, T. Endo, B.-C. Ho, Organic underlayers for EUV lithography, J. Photopolym. Sci. Technol. 21 (2008) 451–455.
[43] Chris Mack, Fundamental Principles of Optical Lithography, John Wiley, West Sussex, 2007.
[44] C.-T. Lee, N.D. Jarnagin, M. Wang, K.E. Gonsalves, J.M. Roberts, W. Yueh, C.L. Henderson, Fundamental studies of the properties of photoresists based on resins containing polymer-bound photoacid generators, Proc. SPIE 6153 (2006), 61532E-1-11.
[45] T.H. Fedynyshyn, R.B. Goodman, J. Roberts, Polymer matrix effects on acid generation, Proc. SPIE 6923 (2008), 692319-1-12.
[46] C.R. Szmanda, R. Kavanagh, J. Bohland, J. Cameron, P. Trefonas, R. Blacksmith, A simple method for measuring acid generation quantum efficiency at 193 nm, Proc. SPIE 3678 (1999) 157–166.